

TTMBA: Towards Text To Multiple Sources Binaural Audio Generation

Yuxuan He¹, Xiaoran Yang¹, Ningning Pan², Gongping Huang¹

¹School of Electronic Information, Wuhan University, Wuhan, Hubei, China

²School of Computing and Artificial Intelligence, Southwestern University of Finance and Economics, Chengdu, Sichuan, China

yuxuanhe@whu.edu.cn, yxr888@whu.edu.cn, nnpn@swufe.edu.cn, gongpinghuang@whu.edu.cn

Abstract

Most existing text-to-audio (TTA) generation methods produce mono outputs, neglecting essential spatial information for immersive auditory experiences. To address this issue, we propose a cascaded method for text-to-multisource binaural audio generation (TTMBA) with both temporal and spatial control. First, a pretrained large language model (LLM) segments the text into a structured format with time and spatial details for each sound event. Next, a pretrained mono audio generation network creates multiple mono audios with varying durations for each event. These mono audios are transformed into binaural audios using a binaural rendering neural network based on spatial data from the LLM. Finally, the binaural audios are arranged by their start times, resulting in multisource binaural audio. Experimental results demonstrate the superiority of the proposed method in terms of both audio generation quality and spatial perceptual accuracy.

Index Terms: Text to binaural audio generation, temporal control, spatial control, binaural audio rendering, multisource

1. Introduction

With the rise of rapid technological innovation, the demand for high-fidelity binaural audio generation has surged in fields such as virtual reality (VR), augmented reality (AR), and mixed-reality systems, particularly for education and entertainment. While deep generative models have advanced audio generation, previous research has primarily focused on mono audio, limiting their effectiveness in scenarios requiring spatial acoustic signatures. In recent years, extensive research has been conducted, and significant progress has been achieved in this field. For instance, DiffSound [1], the first diffusion-based audio generation model, uses a pre-trained VQ-VAE [2] to map mel-spectrograms into discrete tokens, which are generated with a diffusion model. AudioGen [3] adopts a similar VQ-VAE with an autoregressive model in a discrete waveform space. In contrast, AudioLDM [4, 5] employs a continuous latent diffusion model (LDM) [8], yielding better audio quality. While these models effectively control audio duration, they face challenges with multisource audio control, particularly in scenarios requiring precise spatial accuracy.

To address these challenges, recent studies have focused on improving temporal and spatial control in audio generation. Make-An-Audio 2 [6] and TangoFlux [7] prioritize temporal information for variable-length audio generation. Make-An-Audio 2 uses an LLM and temporal encoder for coherent audio

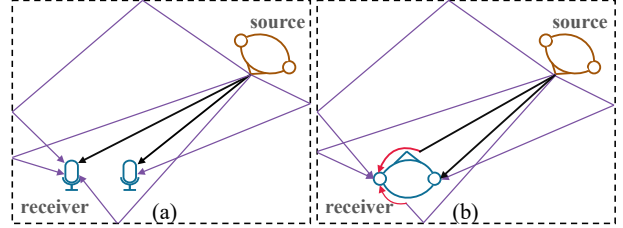


Figure 1: Illustration of acoustic propagation models: (a) Conventional geometric acoustic simulation based solely on room impulse responses; (b) Binaural modeling incorporating listener-specific cues.

generation but incurs high computational costs due to LDM. TangoFlux, a lightweight model for duration control, generates binaural audio by duplicating single-channel recordings, resulting in nearly identical outputs and lacking spatial control through text. To enhance spatial accuracy, we first utilize TangoFlux and subsequently apply binaural rendering with directional cues. BEWO [33] is a latent diffusion model that utilizes text embedding and azimuth information to generate spatial audio. Similarly, Immersive Diffusion [32] combines ELSA [31] with the Diffusion Transformer to produce spatial audio. Both models accept text inputs and generate spatial audio, but they lack precise temporal control and neglect listener anatomy, both of which are essential for authentic binaural perception.

Another class of methods that has garnered significant attention involves rendering mono audio to binaural audio. Traditional simulators, such as Pyroomacoustics [12] efficiently model acoustic propagation between sources and receivers, as shown in Fig. 1 (a). However, these methods mainly focus on room impulse responses (RIRs) and neglect crucial factors such as the listener’s pinnae, head, and torso, all of which are essential for authentic binaural perception [22]. To address this limitation, Head Related Transfer Functions (HRTF) and Binaural Room Transfer Functions (BRTF) model these cues [23]. The NIIRF framework [11] approximates direction-dependent HRTF coefficients with cascaded IIR filters but suffers from spectral errors. Neural networks like BinauralGrad [10] and NFS [13] generate binaural audio, with NFS excelling in both static and dynamic scenarios in the Fourier space. These methods account for the listener’s anatomy, as shown in Fig. 1 (b).

In this paper, we propose a text-to-multisource binaural audio generation model (TTMBA)¹ that synthesizes binaural audio with controllable spatial (azimuth, elevation, distance) and temporal (duration, start time) attributes. The model first employs a pre-trained large language model (LLM) to extract source information, followed by an audio generation network

This work was supported in part by the National Natural Science Foundation of China (NSFC) under Grant 62471340 and in part by the Guangdong Basic and Applied Basic Research Foundation under Grant 2025A1515010226.

¹Demo page: <https://25219.github.io/1.github.io/>

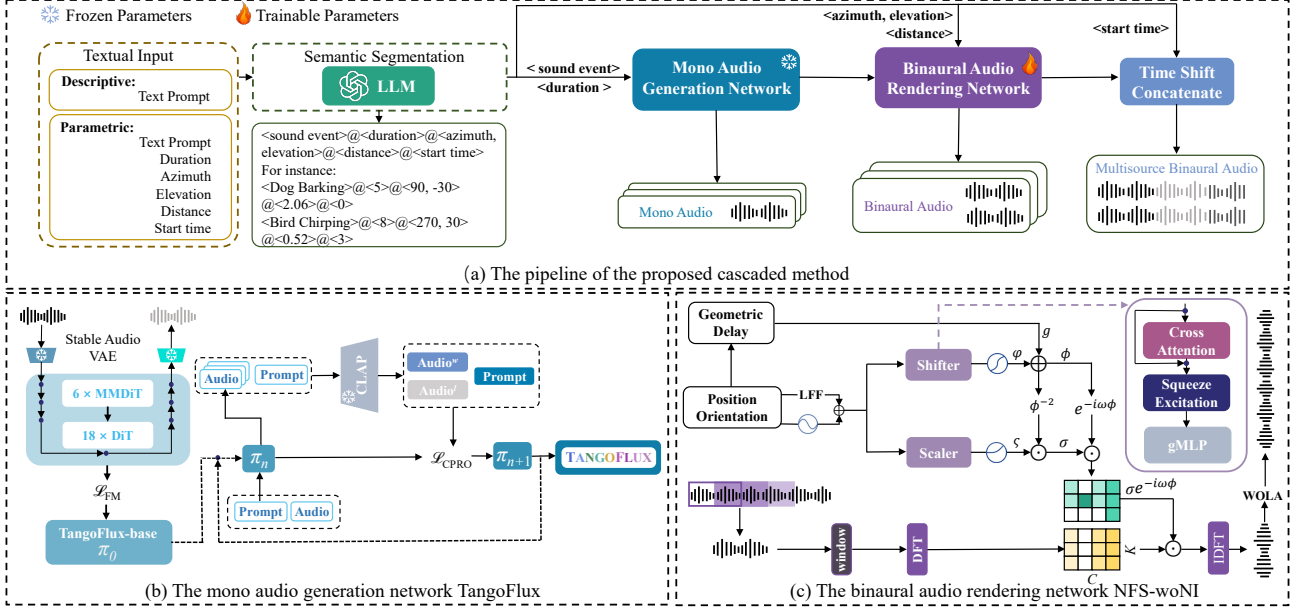


Figure 2: The framework of the proposed text-to-multisource binaural audio generation network.

that synthesizes individual mono streams, and a binaural rendering network simulates directional effects. The contributions of this work include:

- The first text-conditioned binaural audio generation model with control over duration, start time, and location.
- The use of a LLM to extract source location from text, relying on physical principles when cues are absent.
- The developed method achieves strong performance with low computational cost in both quantitative and perceptual evaluations.

2. Method

This work proposes a cascaded pipeline for generating multi-source, duration-controllable binaural audio. It uses a large language model (LLM), GPT-4o², to segment descriptive or parametric text descriptions into multiple sets of structured data in a standard format of `<sound event>@<duration>@<azimuth, elevation>@<distance>@<start time>`, inferring spatial details through commonsense reasoning when position description is missing (e.g., Dog barking typically comes from the downside of human). Sound events and durations are used in TangoFlux³ to generate mono audios, while azimuth, elevation, and distance information guide binaural rendering to produce spatially accurate binaural audio. Finally, these binaural audios are rearranged into one output based on the start time. The pipeline is shown in Fig. 2 (a).

2.1. Text to Mono Audio Generation

We adopt TangoFlux for mono audio generation. As shown in Fig. 2 (b), the text-to-mono audio generation network incorporates a unique combination of 6 Multimodal Diffusion Transformer (MMDiT) [15] and 18 Diffusion Transformer (DiT) [14] blocks, which is conditioned on both text embedding and duration embedding to generate high-quality audio. Initially, a variational autoencoder (VAE) is employed to encode the latent

representations of audio, guiding the network to learn a rectified flow trajectory. Throughout the training process, the VAE is kept frozen.

Given a latent representation \mathbf{x}_1 of an audio sample encoded by the VAE and a noise input $\mathbf{x}_0 \sim \mathcal{N}(\mathbf{0}, \mathbf{I})$, we construct an intermediate state \mathbf{x}_t for $t \in [0, 1]$, where t denotes the flow matching timestep. The network learns to predict a velocity, $\mathbf{v}_t = \frac{d\mathbf{x}_t}{dt}$, guiding \mathbf{x}_t toward the target \mathbf{x}_1 . Rectified flows (RFs) [16] are then applied to transform the noise distribution into the target distribution, following straight-line trajectories. The model \mathbf{u} , where the parameters are denoted as θ , is trained to directly regress the predicted velocity $\mathbf{u}(\mathbf{x}_t, t; \theta)$ toward the ground-truth velocity \mathbf{v}_t , according to the loss function:

$$\mathcal{L}_{\text{FM}} = \mathbb{E}_{\mathbf{x}_1, \mathbf{x}_0, t} \|\mathbf{u}(\mathbf{x}_t, t; \theta) - \mathbf{v}_t\|^2. \quad (1)$$

The network is first pretrained as the initial base model π_0 . Subsequently, CLAP-Ranked Preference Optimization (CRPO) is leveraged to refine the model iteratively, which aligns checkpoint π_n into checkpoint π_{n+1} , starting from $n = 0$. Here, the CLAP model functions as a proxy reward model to assess audios according to how well they match the text input. The loss function for preference optimization, $\mathcal{L}_{\text{DPO-FM}}$, is established to optimize the alignment between the generated audio and the given text description, is defined as:

$$\begin{aligned} \mathcal{L}_{\text{DPO-FM}} = & -\mathbb{E}_{t \sim \mathcal{U}(0,1), \mathbf{x}^w, \mathbf{x}^l} \log \sigma \left(-\beta \left(\|\mathbf{u}(\mathbf{x}_t^w, t; \theta) - \mathbf{v}_t^w\|_2^2 \right. \right. \\ & \left. \left. - \|\mathbf{u}(\mathbf{x}_t^l, t; \theta) - \mathbf{v}_t^l\|_2^2 - \left(\|\mathbf{u}(\mathbf{x}_t^w, t; \theta_{\text{ref}}) - \mathbf{v}_t^w\|_2^2 \right. \right. \right. \\ & \left. \left. \left. - \|\mathbf{u}(\mathbf{x}_t^l, t; \theta_{\text{ref}}) - \mathbf{v}_t^l\|_2^2 \right) \right) \right). \end{aligned} \quad (2)$$

where \mathbf{x}_t^w and \mathbf{x}_t^l correspond to the winning and losing audios evaluated by CLAP, respectively, and θ_{ref} denotes the parameters of the current base model.

To mitigate the risk of overoptimization and maintain stable training, the total loss function $\mathcal{L}_{\text{CRPO}}$ integrates the preference optimization loss $\mathcal{L}_{\text{DPO-FM}}$ in (2) with the flow matching loss \mathcal{L}_{FM} in (1). This combination is formulated as:

$$\mathcal{L}_{\text{CRPO}} := \mathcal{L}_{\text{DPO-FM}} + \mathcal{L}_{\text{FM}}. \quad (3)$$

²<https://openai.com/blog/chatgpt>

³<https://github.com/declare-lab/TangoFlux>

This integrated loss function preserves the semantic and structural integrity of the generated audio while refining preference rankings, resulting in a balanced and resilient optimization. With iterative alignment, a hybrid architecture, and rectified flow, the network generates high-quality, tailored audio that aligns accurately with textual prompts and specified lengths.

2.2. Mono to Binaural Audio Rendering

As illustrated in Fig. 2 (c), the Binaural Audio Rendering Network converts mono audio into binaural audio using Fourier transform theories. When sound propagates, delays and energy changes occur due to attenuation and absorption, which correspond to phase shifts and magnitude reductions in the Fourier domain. The Discrete Fourier Transform (DFT) is applied to the mono signal to compute its frequency-domain representation, where $\omega_k = \frac{2\pi k}{K}$, with $k \in \{0, 1, \dots, K-1\}$ and $\mathbf{X} \in \mathbb{C}^K$. The Fourier shift theorem relates temporal shifts to linear phase shifts, enabling the network to render sound propagation effects like delays and energy alterations accurately.

Building on this, the network aims to predict the magnitude reductions $\sigma \in \mathbb{R}^{C \times K}$ and phase shifts $\phi \in \mathbb{R}^{C \times K}$, where C represents the number of channels for the left (L) and right (R) ears, respectively. Subsequently, the network output, i.e., $\hat{\mathbf{X}}_L(k)$ and $\hat{\mathbf{X}}_R(k)$, are obtained by applying these predicted magnitude scales and phase shifts to the mono spectrum $\mathbf{X}(k)$:

$$\begin{aligned}\hat{\mathbf{X}}_L(k) &= \sum_{c=0}^{C-1} \sigma_L(c, k) e^{-i\omega_k \phi_L(c, k)} \mathbf{X}(k), \\ \hat{\mathbf{X}}_R(k) &= \sum_{c=0}^{C-1} \sigma_R(c, k) e^{-i\omega_k \phi_R(c, k)} \mathbf{X}(k).\end{aligned}\quad (4)$$

The network takes three inputs: mono audio, the source’s position with orientation, and frame-wise geometric delay. The position $\langle \text{azimuth}, \text{elevation} \rangle$ and $\langle \text{distance} \rangle$ are transformed into a spatial position $p \in \mathbb{R}^3$ and orientation $q \in \mathbb{R}^4$, while geometric delay g is calculated from direct-path distances, as shown in Fig. 1. The mono audio is segmented and windowed with a Hanning window. Position and orientation are encoded using sinusoidal encoding and learned Fourier features (LFF). Two parallel modules, *Scaler* and *Shifter*, predict spectral magnitude coefficients and phase offsets. Both modules use cross-attention [24], squeeze-and-excitation [25], and gMLP [26] to encode spatial and orientational information. The outputs pass through nonlinear activation functions, ς (strictly positive) and φ (capped under half the frame length).

The geometric delay g computed from the warp field is added to φ for each frame, yielding $\phi = \varphi + g$. To ensure that energy is inversely proportional to the square of the distance, we normalize ς by dividing it element-wise by ϕ^2 , resulting in the scale parameter $\sigma = \varsigma \odot \phi^{-2}$. We then compute the frame-wise multichannel spectrum $\sigma e^{(-i\omega\phi)}$, which is multiplied with the source in the Fourier domain, as shown in (4). Next, IDFT is applied to $\hat{\mathbf{X}} \in \mathbb{C}^{C \times K}$, and the channels are linearly combined into a single stream. The final output $\hat{\mathbf{x}}$ is generated using a weighted overlap-add (WOLA) synthesis method, without ambient noise injection to enhance quality and mimic real-world binaural recordings, which differentiates it from the initial NFS. This network is referred to as NFS-woNI.

To ensure the generated binaural audio closely matches the target signal \mathbf{y} , the loss function of the network is defined as:

$$\begin{aligned}\mathcal{L}(\hat{\mathbf{x}}, \mathbf{y}) &= \lambda_1 \|\hat{\mathbf{x}} - \mathbf{y}\|_2 + \lambda_2 \|\angle \hat{\mathbf{X}} - \angle \mathbf{Y}\|_1 \\ &+ \lambda_3 \|\text{IID}(\hat{\mathbf{x}}) - \text{IID}(\mathbf{y})\|_2 + \lambda_4 \text{MRSTFT}(\hat{\mathbf{x}}, \mathbf{y}),\end{aligned}\quad (5)$$

where IID quantifies the interaural intensity difference, and MRSTFT [17] represents the multi-resolution short-time Fourier transform loss. The four components in (5) are denoted as ℓ_2 , \mathcal{L}_{phs} , \mathcal{L}_{IID} , and $\mathcal{L}_{\text{STFT}}$, respectively.

3. Experimental Setup

3.1. Datasets and Baselines

To evaluate the quality of the generated mono audios, we conduct experiments using the test set of the AudioCaps dataset [18], which consists of 4,368 audio-text pairs. Each audio clip is 10 seconds long with a 16 kHz sampling rate. For baseline comparisons, we choose AudioLDM and Make-An-Audio 2. Specifically, we use the improved version of AudioLDM, AudioLDM.16k_crossattn.t5, as our selected checkpoint. To ensure fair comparison of duration-controllable audio generation, all audio clips are uniformly truncated or padded to 8 seconds, preserving as much audio information as possible.

As for the binaural audio generation, the binaural rendering network is trained utilizing the Binaural Speech Benchmark Dataset [27], which contains approximately 2 hours of mono-binaural paired audio data recorded on a KEMAR dummy head. For testing, we employ the CIPIC dataset [19], selecting two sets of HRTFs also recorded on a KEMAR dummy head to convolve with the generated mono audio, creating reference audios for the next stage. These reference audios serve as the benchmark for calculating both the objective and subjective metrics of our proposed method and the baselines. We compare the NFS-woNI with Pyroomacoustics, NIIRF, and BinauralGrad, each of which takes the generated mono audio as input. These methods are referred to as TangoFlux-NFS-woNI, TangoFlux-Pyroom, TangoFlux-NIIRF, and TangoFlux-BinauralGrad, respectively.

3.2. Training Details

We use the pre-trained TangoFlux model to generate mono audios. When rendering binaural audios, both the channel count C and the dimensions for sinusoidal encoding are set to 128. The model is refined using the RAdam optimizer [20] over 16 training epochs, employing a batch size of 6. The initial learning rate is set to 10^{-3} and is decayed by a factor of 0.9 at the end of each epoch. The parameters in (5) are as follows: $\lambda_1 = 10^3$, $\lambda_3 = 10^1$, and $\lambda_2 = \lambda_4 = 1$. Notably, the network is trained without noise injection to preserve audio quality—a slight modification compared to the NFS.

4. Results

4.1. Mono Audio Generation Evaluation

We assess the generated audio using both objective and subjective metrics. Objective metrics include Fréchet Distance (FD) [28], Kullback-Leibler divergence (KL) [30], Inception Score (IS) [29], and CLAP score [9]. FD measures similarity to target audio, KL quantifies differences in acoustic event posteriors, IS evaluates diversity and specificity, and CLAP score calculates cosine similarity between audio embeddings and their textual descriptions. Lower FD and KL values indicate better alignment, while higher IS and CLAP scores reflect greater diversity and stronger text-audio alignment. For subjective evaluation, participants with normal hearing rate the mono audios using Mean Opinion Score (MOS) for audio quality (MOS-Q) and text-audio alignment (MOS-F).

We first compare the performance of TangoFlux in the first

Table 1: Comparison of different TTA models and the proposed method evaluated by 1 channel across various metrics. The highest score for each metric is marked with an asterisk (\cdot^*) and the second highest score is marked with a dagger (\cdot^\dagger).

Method	FD \downarrow	KL \downarrow	IS \uparrow	CLAP \uparrow	MOS-Q \uparrow	MOS-F \uparrow	Inference Time (s) \downarrow
AudioLDM	21.06	1.43	9.89	0.54	3.07	2.61	41.55
Make-An-Audio 2	13.43*	1.38	10.58	0.55	3.36	3.32	27.77
TangoFlux	17.74\dagger	1.33*	13.94*	0.61*	4.64*	4.79*	2.22*
TangoFlux-NFS-woNI	17.81	1.35\dagger	11.79\dagger	0.58\dagger	4.57\dagger	4.57\dagger	2.58\dagger

Table 2: Comparison of different binaural audio rendering methods evaluated by 2 channels across various metrics. The highest score for each metric is marked with an asterisk (\cdot^*) and the second highest score is marked with a dagger (\cdot^\dagger).

Method	ℓ_2 \downarrow	\mathcal{L}_{mag} \downarrow	\mathcal{L}_{phs} \downarrow	$\mathcal{L}_{\text{STFT}}$ \downarrow	PESQ \uparrow	MOS-Q \uparrow	MOS-P \uparrow
TangoFlux-Pyroom	0.10	0.92	1.57\dagger	2.05	2.58*	4.23\dagger	3.48
TangoFlux-NIIRF	0.12	0.72	1.57*	1.89\dagger	2.25	4.00	2.86
TangoFlux-BinauralGrad	0.06*	0.67\dagger	1.57	3.37	1.77	3.19	3.95\dagger
TangoFlux-NFS-woNI	0.08\dagger	0.57*	1.58	1.61*	2.43\dagger	4.71*	4.57*

stage with two other TTA models, namely AudioLDM and Make-An-Audio 2. To verify that the processing in the second stage does not compromise audio quality, we also evaluate metrics of the binaural audio output. Specifically, one channel is extracted from the binaural audio for metric assessment. Table 1 demonstrates that TangoFlux outperforms other TTA models across all metrics, with a particularly significant reduction in the average inference time per audio sample, among which all inference times are computed on the NVIDIA GeForce RTX 4090 GPU. Additionally, the result indicate that the audio generated by the proposed TangoFlux-NFS-woNI exhibits similar performance to TangoFlux, with minimal distortion in audio quality due to binaural audio rendering. The MOS-Q and MOS-F scores confirm that the audio generated by the proposed method maintains high quality and accurate text-audio alignment.

4.2. Binaural Audio Rendering Evaluation

In our evaluation of binaural audio, we employ both objective and subjective metrics to comprehensively assess the quality and spatial accuracy of the generated audio. For the objective evaluation, we utilize five metrics: ℓ_2 , \mathcal{L}_{mag} , \mathcal{L}_{phs} , $\mathcal{L}_{\text{STFT}}$, and (PESQ) [21], where \mathcal{L}_{mag} quantifies the spectral magnitude error between the generated and reference audio, while ℓ_2 , \mathcal{L}_{phs} , and $\mathcal{L}_{\text{STFT}}$ are defined in (5). PESQ measures the perceptual quality of the audio. Subjectively, we use MOS-Q and MOS-P to assess overall audio quality and spatial accuracy, respectively. For MOS-P, listeners compare the reference audio with four generated audios, scoring each based on the perceived similarity of the sound source location to the reference.

We then evaluate the performance of different binaural audio rendering methods in the second stage. As shown in Table 2, the proposed TangoFlux-NFS-woNI obtains the best \mathcal{L}_{mag} and $\mathcal{L}_{\text{STFT}}$ scores and the second-best ℓ_2 and PESQ scores across objective metrics. It also outperforms all other methods in subjective metrics, MOS-Q and MOS-P, which confirm that the binaural audios generated by TangoFlux-NFS-woNI maintain high quality and accurately preserves source positioning. In contrast, TangoFlux-BinauralGrad demonstrates good performance in MOS-P but get low score in MOS-Q, indicating the model is not robust in static sound source. TangoFlux-Pyroom performs well in MOS-Q but shows not well in MOS-P, indicating binaural audio requires further consideration of spectral distortions resulting from interactions with the listener’s pinnae,

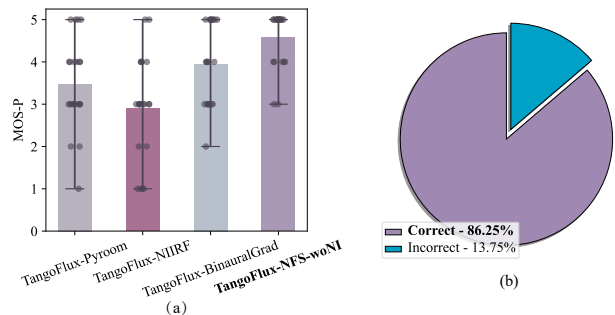


Figure 3: Subjective evaluations of the generated binaural audio: (a) The comparison of MOS-P distribution and average scores across the four methods; (b) Percentage of correct answers in the direction perception test.

head, and torso. The distribution of MOS-P collected from the audience is shown in the Fig. 3 (a), where the height of each bar represents the average score of the corresponding method, and each scatter point represents an individual rating.

We also evaluate the accuracy of the sound source directions perceived by listeners based on the binaural outputs of TangoFlux-NFS-woNI. Specifically, listeners are asked to identify the direction of two sound sources by selecting: 1) left or right, 2) front or rear, and 3) above or below (e.g., dog barking is left, rear, below; bird chirping is right, front, above). As shown in Fig. 3 (b), the results demonstrate that most participants accurately identified the sound source directions, achieving an 86.25% accuracy rate. This confirms the capability of the proposed method to render sound sources in the desired spatial directions.

5. Conclusion

We propose a cascaded lightweight neural network for text-to-multisource binaural duration controllable audio generation. The model uses GPT-4o to extract sound events and sources from text input, TangoFlux to generate mono audios, a Fourier transform network to render high quality binaural audios. Experimental results confirm that the proposed method generate high quality binaural audio with both temporal and spatial control, specifically, audio quality perform best and over 85% accuracy in source locations according to user-defined conditions.

6. References

- [1] D. Yang, J. Yu, H. Wang, W. Wang, C. Weng, Y. Zou, and D. Yu, "DiffSound: Discrete diffusion model for text-to-sound generation," *IEEE/ACM Transactions on Audio, Speech, and Language Processing*, vol. 31, pp. 1720–1733, 2023.
- [2] A. van den Oord, O. Vinyals, and K. Kavukcuoglu, "Neural discrete representation learning," in *Proceedings of the International Conference on Neural Information Processing Systems (NeurIPS)*, 2017, pp. 6309–6318.
- [3] F. Kreuk, G. Synnaeve, A. Polyak, U. Singer, A. Défossez, J. Copet, D. Parikh, Y. Taigman, and Y. Adi, "AudioGen: Textually guided audio generation," in *Proceedings of the International Conference on Learning Representations (ICLR)*, 2023.
- [4] H. Liu, Z. Chen, Y. Yuan, X. Mei, X. Liu, D. Mandic, W. Wang, and M. D. Plumbley, "AudioLDM: Text-to-audio generation with latent diffusion models," in *Proceedings of the International Conference on Machine Learning (ICML)*, 2023, pp. 21 450–21 474.
- [5] H. Liu, Y. Yuan, X. Liu, X. Mei, Q. Kong, Q. Tian, Y. Wang, W. Wang, Y. Wang, and M. D. Plumbley, "AudioLDM 2: Learning holistic audio generation with self-supervised pretraining," *IEEE/ACM Transactions on Audio, Speech, and Language Processing*, vol. 32, pp. 2871–2883, 2024.
- [6] J. Huang, Y. Ren, R. Huang, D. Yang, Z. Ye, C. Zhang, J. Liu, X. Yin, Z. Ma, and Z. Zhao, "Make-An-Audio 2: Temporal-enhanced text-to-audio generation," *arXiv*, vol. abs/2305.18474, 2023.
- [7] C. Hung, N. Majumder, Z. Kong, A. Mehrish, R. Valle, B. Catanzaro, and S. Poria, "TangoFlux: Super fast and faithful text to audio generation with flow matching and clap-ranked preference optimization," *arXiv*, vol. abs/2412.21037, 2024.
- [8] R. Rombach, A. Blattmann, D. Lorenz, P. Esser, and B. Ommer, "High-resolution image synthesis with latent diffusion models," in *Proceedings of the IEEE/CVF Conference on Computer Vision and Pattern Recognition (CVPR)*, June 2022, pp. 10 684–10 695.
- [9] B. Elizalde, S. Deshmukh, M. A. Ismail, and H. Wang, "CLAP learning audio concepts from natural language supervision," in *Proceedings of the IEEE International Conference on Acoustics, Speech and Signal Processing (ICASSP)*, 2023, pp. 1–5.
- [10] Y. Leng, Z. Chen, J. Guo, H. Liu, J. Chen, X. Tan, D. P. Mandic, L. He, X. Li, T. Qin, S. Zhao, and T. Liu, "BinauralGrad: A two-stage conditional diffusion probabilistic model for binaural audio synthesis," in *Proceedings of the International Conference on Neural Information Processing Systems (NeurIPS)*, 2022.
- [11] Y. Masuyama, G. Wichern, F. G. Germain, Z. Pan, S. Khurana, C. Hori, and J. Le Roux, "NIIRF: Neural IIR filter field for HRTF upsampling and personalization," in *Proceedings of the IEEE International Conference on Acoustics, Speech and Signal Processing (ICASSP)*, 2024, pp. 1016–1020.
- [12] R. Scheibler, E. Bezzam, and I. Dokmanić, "Pyroomacoustics: A python package for audio room simulation and array processing algorithms," in *Proceedings of the IEEE International Conference on Acoustics, Speech and Signal Processing (ICASSP)*, 2018, pp. 351–355.
- [13] J. Woo Lee and K. Lee, "Neural fourier shift for binaural speech rendering," in *Proceedings of the IEEE International Conference on Acoustics, Speech and Signal Processing (ICASSP)*, 2023, pp. 1–5.
- [14] W. Peebles and S. Xie, "Scalable diffusion models with transformers," in *Proceedings of the IEEE/CVF International Conference on Computer Vision (ICCV)*, 2023, pp. 4172–4182.
- [15] P. Esser, S. Kulal, A. Blattmann, R. Entezari, J. Müller, H. Saini, Y. Levi, D. Lorenz, A. Sauer, F. Boesel, D. Podell, T. Dockhorn, Z. English, and R. Rombach, "Scaling rectified flow transformers for high-resolution image synthesis," in *Proceedings of the International Conference on Machine Learning (ICML)*, 2024.
- [16] X. Liu, C. Gong, and Q. Liu, "Flow straight and fast: Learning to generate and transfer data with rectified flow," in *Proceedings of the International Conference on Learning Representations (ICLR)*, 2023.
- [17] R. Yamamoto, E. Song, and J.-M. Kim, "Parallel wavegan: A fast waveform generation model based on generative adversarial networks with multi-resolution spectrogram," in *Proceedings of the IEEE International Conference on Acoustics, Speech and Signal Processing (ICASSP)*, 2020, pp. 6199–6203.
- [18] C. D. Kim, B. Kim, H. Lee, and G. Kim, "Audiocaps: Generating captions for audios in the wild," in *Proceedings of the Conference of the North American Chapter of the Association for Computational Linguistics: Human Language Technologies (NAACL-HLT)*, 2019, pp. 119–132.
- [19] V. Algazi, R. Duda, D. Thompson, and C. Avendano, "The CIPIC HRTF database," in *Proceedings of the IEEE Workshop on Applications of Signal Processing to Audio and Acoustics (WASPAA)*, 2001, pp. 99–102.
- [20] L. Liu, H. Jiang, P. He, W. Chen, X. Liu, J. Gao, and J. Han, "On the variance of the adaptive learning rate and beyond," in *Proceedings of the International Conference on Learning Representations (ICLR)*, 2020.
- [21] A. Rix, J. Beerends, M. Hollier, and A. Hekstra, "Perceptual evaluation of speech quality (PESQ)-a new method for speech quality assessment of telephone networks and codecs," in *Proceedings of the IEEE International Conference on Acoustics, Speech and Signal Processing (ICASSP)*, vol. 2, 2001, pp. 749–752.
- [22] D. Wright, J. H. Hebrank, and B. Wilson, "Pinna reflections as cues for localization," *The Journal of the Acoustical Society of America*, vol. 56, no. 3, pp. 957–962, 1974.
- [23] F. L. Wightman and D. J. Kistler, "Headphone simulation of free-field listening. I: Stimulus synthesis," *The Journal of the Acoustical Society of America*, vol. 85, no. 2, pp. 858–867, 1989.
- [24] A. Vaswani, N. Shazeer, N. Parmar, J. Uszkoreit, L. Jones, A. N. Gomez, Ł. Kaiser, and I. Polosukhin, "Attention is all you need," in *Proceedings of the International Conference on Neural Information Processing Systems (NeurIPS)*, 2017, pp. 5998–6008.
- [25] J. Hu, L. Shen, and G. Sun, "Squeeze-and-excitation networks," in *Proceedings of the IEEE conference on computer vision and pattern recognition (CVPR)*, 2018, pp. 7132–7141.
- [26] H. Liu, Z. Dai, D. So, and Q. V. Le, "Pay attention to MLPs," *Advances in Neural Information Processing Systems*, vol. 34, pp. 9204–9215, 2021.
- [27] A. Richard, D. Markovic, I. D. Gebru, S. Krenn, G. A. Butler, F. Torre, and Y. Sheikh, "Neural synthesis of binaural speech from mono audio," in *International Conference on Learning Representations*, 2020.
- [28] A. L. Cramer, H.-H. Wu, J. Salamon, and J. P. Bello, "Look, listen, and learn more: Design choices for deep audio embeddings," in *Proceedings of the IEEE International Conference on Acoustics, Speech and Signal Processing (ICASSP)*, 2019, pp. 3852–3856.
- [29] T. Salimans, I. Goodfellow, W. Zaremba, V. Cheung, A. Radford, and X. Chen, "Improved techniques for training GANs," in *Proceedings of the International Conference on Neural Information Processing Systems*, 2016, pp. 2234–2242.
- [30] S. Kullback and R. A. Leibler, "On information and sufficiency," *Annals of Mathematical Statistics*, vol. 22, pp. 79–86, 1951.
- [31] B. Devnani, S. Seto, Z. Aldeneh, A. Toso, E. Menyaylenko, B. Theobald, J. Sheaffer, and M. Sarabia, "Learning spatially-aware language and audio embeddings," in *Proceedings of the International Conference on Neural Information Processing Systems (NeurIPS)*, 2024, pp. 10–15.
- [32] M. Heydari, M. Souden, B. Conejo, and J. Atkins, "ImmerseDiffusion: A generative spatial audio latent diffusion model," *arXiv*, vol. abs/2410.14945, 2024.
- [33] P. Sun, S. Cheng, X. Li, Z. Ye, H. Liu, H. Zhang, W. Xue, and Y. Guo, "Both Ears Wide Open: Towards language-driven spatial audio generation," *arXiv*, vol. abs/2410.10676, 2024.